Clim. Past Discuss., 10, 3617–3629, 2014
www.clim-past-discuss.net/10/3617/2014/
doi:10.5194/cpd-10-3617-2014

Climate of the Past
Discussions
Open Access

Geothermal evidence of the Late Pleistocene-Holocene orbital forcing (example from the Urals, Russia)

D. Y. Demezhko and A. A. Gornostaeva

Institute of Geophysics UB RAS, Yekaterinburg, Russia

Received: 16 July 2014 – Accepted: 14 August 2014 – Published: 29 August 2014

Correspondence to: D. Y. Demezhko (ddem54@inbox.ru)

Published by Copernicus Publications on behalf of the European Geosciences Union.

Title Page
Abstract | Introduction
Conclusions | References
Tables | Figures
I◀ | ▶I
◀ | ▶
Back | Close
Full Screen / Esc
Printer-friendly Version
Interactive Discussion

Abstract

We use early obtained in the Middle Urals geothermal reconstruction of the ground surface temperature (GST) history to determine the surface heat flux (SHF) history over the past 35 kyr. A new algorithm of GST-SHF transformation was applied to solve this problem. The time scale of geothermal reconstructions has been corrected by comparing the estimated heat flux and annual insolation at the latitude of 60° N. The consistency of SHF and insolation changes on the interval 35–6 kyr BP (the linear correlation coefficient $R = 0.99$) points to orbital factors as the main cause of climatic changes during the Pleistocene–Holocene transition. The amplitude of SHF variations is about 1.3 % of the insolation changes amplitude. The increase of carbon dioxide concentrations lagged by 2–3 kyr from the SHF increase and occurred synchronously with GST changes.

1 Introduction

The role of orbital factors in Pleistocene climatic variations has been studied more than 100 years since Joseph Adhemar, James Croll and Milutin Milankovitch. A popular approach is comparing paleotemperatures reconstructed from proxy data (oxygen isotopes, palynological or others) with theoretically calculated insolation. Some investigators (Peixóto and Oort, 1984; Pielke, 2003; Douglass and Knox, 2012) criticized this approach. They noted that temperature field is not an optimal parameter for climate attribution, particularly for evaluation of climatic reaction on the external radiative forcing. There is a lag between external radiative flux and temperature changes, which is disappeared if we consider the heat content or the surface heat flux changes. The advantage of heat flux estimation over temperature one was not realized in full up to date. Wang and Bras (1999) proposed the integral relation to estimate surface heat flux (SHF) changes from ground surface temperature (GST) variations. A finite-difference approximation of the relation between the GST (represented by a piecewise linear function of temperature), and the SHF was proposed by Beltrami et al. (2002). SHF history reconstructions based on borehole temperature data were made in timescales from several centuries to millennium (Beltrami et al., 2002, 2006; Huang, 2006). Another approach was used in (Majorowicz et al., 2012). Subsurface temperatures were calculated from solar irradiance change using information about climate sensitivity.

In the paper we first present the SHF history for the past 35 kyr obtained from GST early reconstructed on the basis of temperature-depth profile logged in the Urals superdeep borehole (Demezhko and Shchapov, 2001). The recently developed improved algorithm of GST-SHF transformation (Gornostaeva, 2014) was applied to estimate the SHF history.

2 The method

The GST-SHF transformation algorithm is based on the relation between surface heat flux and surface temperature changes according to the Fourier's equation in one dimension:

$$q(0,t) = -\lambda \left. \frac{\partial T(z,t)}{\partial z} \right|_{z=0} \quad (1)$$

where q is SHF, t is time, λ is thermal conductivity, $T(z,t)$ is temperature anomaly at a depth z.

If GST is represented by an expression (Lachenbruch et al., 1982)

$$T(0,t) = D(t)^{\frac{n}{2}} \quad (2)$$

where D is a constant, n is positive integer (or 0) determining the shape of temperature changes, the transient temperature anomaly at any depth is

$$T(z,t) = 2^n \Gamma\left(\frac{1}{2}n+1\right)\ i^n \operatorname{erfc}\frac{z}{\sqrt{4at}} T(0,t) \quad (3)$$

where $a = \frac{\lambda}{\rho C}$ is thermal diffusivity, ρ is density, C is specific heat capacity, $i^n \operatorname{erfc}(\alpha)$ is the nth repeated integral of the error function of α and $\Gamma(\beta)$ is gamma-function of argument β. Differentiation of Eq. (3) yields SHF

$$q(0,t) = \frac{\Gamma\left(\frac{1}{2}n+1\right)}{\Gamma\left(\frac{1}{2}n+\frac{1}{2}\right)} \cdot \frac{\lambda}{\sqrt{at}} \cdot T(0,t) \qquad (4)$$

Note that the ratio $E = \lambda/(a)^{-1/2}$ represents the rock's thermal effusivity (thermal inertia) characterizing the rate of heat exchange at the surface.

We approximate GST history by a sum of temperature changes corresponding to Eq. (2):

$$T_i = T_0 + \sum_{j=1}^{i} D_j (i-j+1)^{\frac{n}{2}} \qquad (5)$$

where i, j are positive integers related with the real time by the equations $t = i \cdot \Delta t$, $t = j \cdot \Delta t$, Δt is uniform time interval. For each addend of this sum

$$T_i = D_i i^{n/2}, \quad q_i = k_n \frac{E}{\sqrt{\Delta t}} D_i i^{\frac{n-1}{2}}, \quad k_n = \frac{\Gamma\left(\frac{1}{2}n+1\right)}{\Gamma\left(\frac{1}{2}n+\frac{1}{2}\right)}. \qquad (6)$$

Using a recurrence equation

$$D_i = (T_i - T_0) - \sum_{j=1}^{i-1} D_j (i-j+1)^{\frac{n}{2}}, \quad i > 1 \qquad (7)$$

one can estimate D_i for each interval of temperature curve and then by the equation

$$q_i = k_n \frac{E}{\sqrt{\Delta t}} \sum_{j=1}^{i} D_j (i-j+1)^{\frac{n-1}{2}} \qquad (8)$$

one can calculate heat flux instantaneous values at the end of interval. The SHF history reconstruction will be more accurate if we calculate the average value of heat flux on the interval and refer it to the midpoint of the interval ($i - 0.5$)

$$\overline{q_{i-0.5}} = q_{i-1} + \frac{2}{n+1}(q_i - q_{i-1}). \tag{9}$$

The GST-SHF transformation algorithm was tested by applying it to harmonic function of surface temperature change. The test showed that approximation of temperature history by the Eq. (5) with $n = 2, 3$ provides the most accurate results. When GST discretization is 6 points per period we obtain the relative error of SHF history estimation equals to 3 %, and given 10 points per period the relative error is less than 1 % (Gornostaeva, 2014). For comparison, the algorithm proposed by Beltrami et al. (2002) under the same discretization conditions provides relative errors equals to 8 % and 3.5 % respectively.

3 GST data and SHF reconstruction

We used temperature history (Demezhko and Shchapov, 2001) early reconstructed from temperature-depth profile logged in the Urals superdeep borehole SG-4 (58°24′ N, 59°44′ E, Middle Urals, Russia) as initial data. The reconstruction of the surface heat flux history was conducted using the algorithm described above with $n = 3$ (see Fig. 1). GST and SHF curves are different in shape. The temperature increase started about 15 kyr BP and after a short break it continued to 1 kyr BP, while the heat flux increase began about 3 kyr earlier. The heat flux reached its maximum of 0.08 W m^{-2} about 8 kyr BP and then it began to decline.

4 The comparison of the SHF with solar insolation

The reconstructed SHF changes are similar to the Northern Hemisphere solar insolation changes that are determined by the variations of the Earth's orbital parameters like eccentricity, inclination and the Earth's axis precession (Fig. 2). However, there is some time shift between insolation and SHF changes. The observed shift can be explained by several reasons. The first one is the influence of inertial climatic factors (feedbacks) translating the external heat flux on the Earth's surface with a certain delay and amplitude attenuation. The second reason is an overestimation of the effective thermal diffusivity that determines the rate of climatic signal propagation into the depth and therefore the time scale of geothermal reconstructions. To synchronize SHF and insolation (ΔI) time series it is necessary to correct the initial value of thermal diffusivity (and time scale respectively) to maximize the correlation between them. Note that the direct comparison of these series is not so correct. The insolation temporal resolution is constant while SHF resolution power decreases back in time. A minimal resolved interval of geothermal reconstruction is approximately $2 \cdot t^*/3$ where t^* is time before present (Demezhko and Shchapov, 2001). The procedure of averaging in uneven running windows was proposed (Demezhko and Solomina, 2009) to modify the curve to a form comparable with the geothermal one. The insolation curve for the latitude of 60° N smoothed according to the resolution power of geothermal method is presented in Fig. 2b. A maximum correlation between SHF history and smoothed insolation is achieved by increasing SHF dates by 1.4 times. It corresponds to the thermal diffusivity decrease from initial value of $a = 1.0 \times 10^{-6}\,\mathrm{m^2\,s^{-1}}$ to $0.71 \times 10^{-6}\,\mathrm{m^2\,s^{-1}}$.

Linear regression analysis of q and ΔI from 35 to 6 kyr BP showed that change of insolation on $1\,\mathrm{W\,m^{-2}}$ produces an additional surface heat flux equals to $0.013\,\mathrm{W\,m^{-2}}$ (the linear correlation coefficient $R = 0.99$). So, at least until 6 kyr BP the reconstructed heat flux variability was almost completely determined by orbital forcing. At that only a small portion of insolation changes (about 1.3 %) was spent to the increase of the lithosphere heat content. The ratio $\Delta q/\Delta I$ may be considered as a dimensionless measure of climate sensitivity of the region under study to long-term orbital forcing variations.

Taking the climatically caused SHF before 35 kyr BP equals to 0 W m^{-2} and integrating it with respect to time we estimate changes in heat content. This value characterizes the additional amount of heat adsorbed in a rock column having a cross-sectional area of 1 m^2 and limited by the depth of thermal anomaly penetration (i.e. by a few kilometers). Until 15 kyr BP a total heat balance was negative. A minimum value of heat content of –3.5 TJ m^{-2} with respect to the reference value at 35 kyr BP was found about 20 kyr BP. From this moment the heat flux became positive. For the next 14 kyr (20–6 kyr BP) the heat content increased to 22.0 TJ m^{-2}. For comparison, during the period of modern warming (1765–2000), heat content of the continental lithosphere increased by 0.1 TJ m^{-2} (calculated using data from Beltrami, 2002).

5 The comparison of the SHF with CO$_2$ changes

Another source of the additional radiative forcing during the Pleistocene–Holocene transition could be greenhouse effect caused by the increase of carbon dioxide concentration in the atmosphere (see Shakun et al., 2012 and references therein). An additional downward heat flux necessarily would contributes to SHF changes. Figure 3 shows geothermal reconstructions of surface temperatures and heat fluxes from the borehole SG-4 (on the time scale corrected after SHF-insolation synchronization) and carbon dioxide concentration changes in Antarctic ice cores (Blunier et al., 1998; Indermühle et al., 1999a, b; Smith, 1999; Barnola et al., 2003; Pedro et al., 2012). Despite the substantial dispersion of CO$_2$ estimations, a character and a chronology of CO$_2$ concentration changes are much closer to temperature changes rather than to heat flux variations. It may means no significant contribution of CO$_2$ forcing to climatically caused heat flux during Pleistocene–Holocene warming.

About 10 kyr BP the increase of carbon dioxide concentration was replaced by its fall which ended about 8 kyr BP. This local minimum is not consistent with either GST or SHF histories. It is possible that the CO_2 decrease was associated with a sharp increase of vegetation absorbing its excess.

6 Conclusions

The reconstruction of the surface heat flux history using data on the past surface temperature changes represents a new instrument for climate analysis. The reconstructed SHF variations and radiative forcing changes may be compared directly because they are expressed in the same units of energy flux ($\mathrm{W\,m^{-2}}$) and there is no time lag in SHF reaction on external radiative forcing changes. The ratio between surface heat flux and external forcing ($\Delta q/\Delta I$) may be considered as an alternative measure of the Earth's climatic sensitivity. The ratio of heat fluxes is a non-dimensional parameter, and additionally depends less on radiative forcing duration by contrast to traditional index of climatic sensitivity representing temperature reaction on the external radiative forcing ($\Delta T/\Delta I$).

The described algorithm of GST-SHF transformation is quite easy to realization and allows estimating of SHF history with high precision.

Using this algorithm, we have first estimated long-term surface heat flux changes in the Urals for the past 35 kyr. The reconstructed SHF variations are almost completely coincides with changes in insolation of Northern Hemisphere on the scale of the last glacial–interglacial cycle. The amplitude of heat flux variations was about 1.3 % of the insolation changes range at the latitude of 60° N. The increase of carbon dioxide concentrations occurred 2–3 thousands of years later than the heat flux increase and synchronously with temperature response.

Acknowledgements. This study was supported by the Russian Foundation for Basic Research (RFBR) within the framework of the scientific projects No. 13-05-00724-a and No. 14-05-31055 mol_a.

References

Barnola, J.-M., Raynaud, D., Lorius, C., and Barkov, N. I.: Historical CO_2 record from the Vostok ice core, available at: http://cdiac.ornl.gov/trends/co2/vostok.html, 2003.

Beltrami, H.: Climate from borehole data: energy fluxes and temperatures since 1500, Geophys. Res. Lett., 29, 26-1–26-4, 2002.

Beltrami, H., Smerdon, J. E., Pollack, H. N., and Huang, S.: Continental heat gain in the global climate system, Geophys. Res. Lett., 29, 8-1–8-3, 2002.

Beltrami, H., Bourlon, E., Kellman, L., and González-Rouco, J. F.: Spatial patterns of ground heat gain in the Northern Hemisphere, Geophys. Res. Lett., 33, L06717, 2006.

Berger, A. and Loutre, M. F.: Insolation values for the climate of the last 10 million of years, Quaternary Sci. Rev., 10, 297–317, 1991.

Demezhko, D. Y. and Shchapov, V. A.: 80 000 years ground surface temperature history inferred from the temperature-depth log measured in the superdeep hole SG-4 (the Urals, Russia), Global Planet. Change, 29, 219–230, 2001.

Demezhko, D. Y. and Solomina, O. N.: Ground surface temperature variations on Kunashir Island in the last 400 years inferred from borehole temperature data and tree-ring records, Dokl. Earth Sci., 426, 628–631, 2009.

Douglass, D. H. and Knox, R. S.: Ocean heat content and Earth's radiation imbalance, II. Relation to climate shifts, Phys. Lett. A, 376, 1226–1229, 2012.

Gornostaeva, A. A.: The calculation algorithm of ground surface heat flux changes from ground temperature changes, Urals Geophysical Herald, 1, 30–39, 2014 (in Russian).

Huang, S.: 1851–2004 annual heat budget of the continental landmasses, Geophys. Res. Lett., 33, L04707, 2006.

Indermühle, A., Monnin, E., Stauffer, B., Stocker, T. F., and Wahlen, M.: Atmospheric CO_2 concentration from 60 to 20 kyr BP from the Taylor Dome ice core, Antarctica, Geophys. Res. Lett., 27, 735–738, 1999a.

Indermühle, A., Stocker, T. F., Joos, F., Fischer, H., Smith, H. J., Wahlen, M., Deck, B., Mastroianni, D., Tschumi, J., Blunier, T., Meyer, R., and Stauffer, B.: Holocene carbon-cycle dynamics based on CO_2 trapped in ice at Taylor Dome, Antarctica, Nature, 398, 121–126, 1999b.

Lachenbruch, A., Sass, J. H., Marshall, B. V., and Mases Jr., T. H.: Permafrost, heat flow, and the geothermal regime at Prudhoe Bay, Alaska, J. Geophys. Res., 87, 9301–9316, 1982.

Majorowicz, J., Scinner, W., and Safanda, J.: Western Canadian Sedimentary Basin temperature–depth transients from repeated well logs: evidence of recent decade subsurface heat gain due to climatic warming, J. Geophys. Eng., 9, 127–137, 2012.

Pedro, J. B., Rasmussen, S. O., and van Ommen, T. D.: Tightened constraints on the time-lag between Antarctic temperature and CO_2 during the last deglaciation, Clim. Past, 8, 1213–1221, doi:10.5194/cp-8-1213-2012, 2012.

Peixóto J. P. and Oort, A. H.: Physics of climate, Rev. Mod. Phys., 56, 365–429, 1984.

Pielke Sr., R. A.: Heat storage within the Earth system, B. Am. Meteorol. Soc., 84, 331–335, 2003.

Shakun, J. D., Clark, P. U., He, F., Marcott, S. A., Mix, A. C., Liu, Z., Otto-Bliesner, B., Schmittner, A., and Bard, E.: Global warming preceded by increasing carbon dioxide concentrations during the last deglaciation, Nature, 484, 49–54, 2012.

Smith, H. J., Fischer, H., Mastroianni, D., Deck, B., and Wahlen, M.: Dual modes of the carbon cycle since the Last Glacial Maximum, Nature, 400, 248–250, 1999.

Wang, J. and Bras, R. L.: Ground heat flux estimated from surface soil temperature, J. Hydrol., 216, 214–226, 1999.

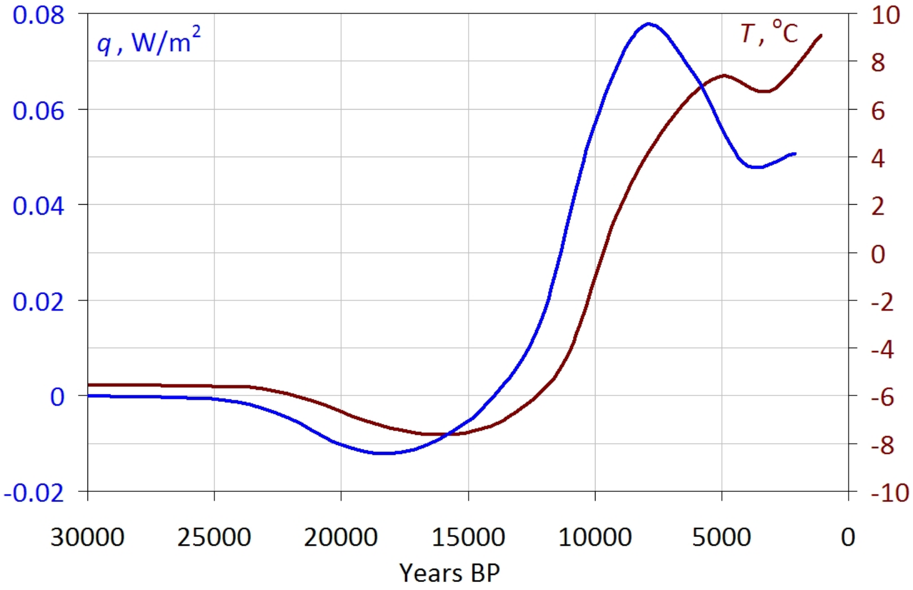

Figure 1. GST history for the Middle Urals $T(t)$ ($a = 1.0 \times 10^{-6}\,\mathrm{m^2\,s^{-1}}$, Demezhko, Shchapov, 2001, brown line) and calculated according to Eqs. (7)–(9) SHF history $q(t)$ ($n = 3$, $E = 2500\,\mathrm{J\,m^{-2}\,K^{-1}\,s^{-1/2}}$, blue line).

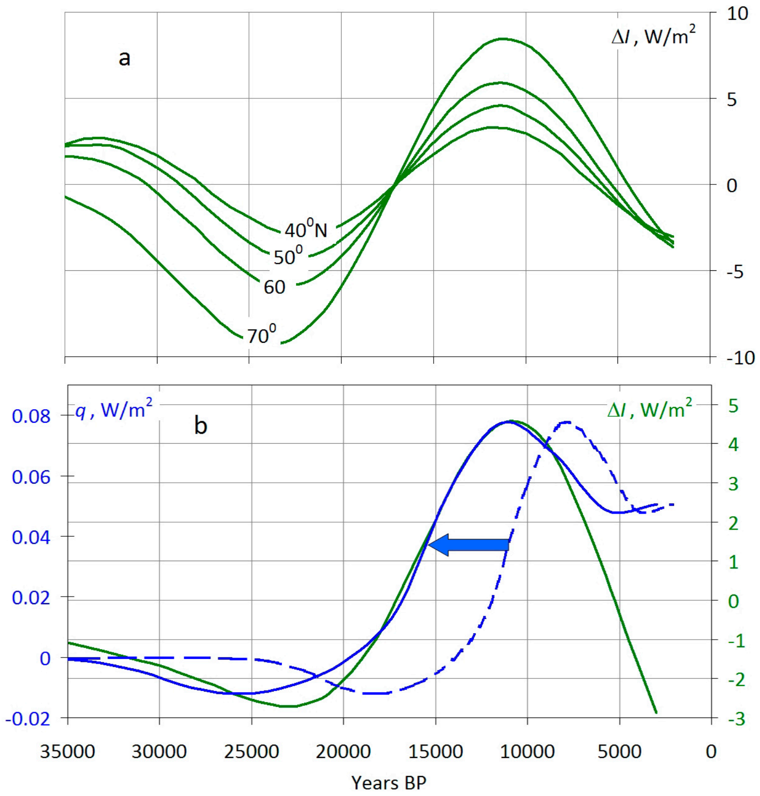

Figure 2. The comparison of SHF history with solar insolation changes in the Northern Hemisphere caused by changes in Earth's orbital parameters and time scale correcting. **(a)** Annual insolation changes $\Delta I(t)$ at the latitudes of 40–70° N (Berger, Loutre, 1991); **(b)** annual solar insolation at the latitude of 60° N smoothed in uneven running windows (green line), SHF history in the initial timescale ($a = 1.0 \times 10^{-6}$ m^2 s^{-1}, blue dashed line) and SHF history in the corrected timescale ($a = 0.71 \times 10^{-6}$ m^2 s^{-1}, blue solid line).

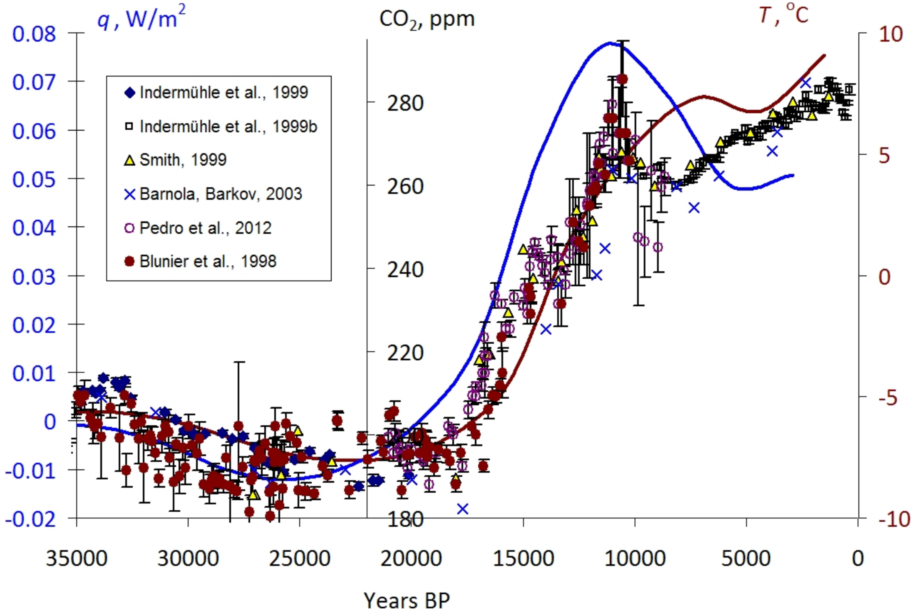

Figure 3. The comparison of GST history $T(t)$ (brown line), SHF history $q(t)$ (blue line) and CO_2 concentration in the Antarctic ice cores (multicolored markers).